Sensory and Motor Systems

The Contributions of Mu-Opioid Receptors on Glutamatergic and GABAergic Neurons to Analgesia Induced by Various Stress Intensities

Yinan Du, Kexin Yu, Chuanting Yan, Chunling Wei, Qiaohua Zheng, Yanning Qiao, Yihui Liu, Jing Han, Wei Ren, and Zhiqiang Liu

Abstract

The endogenous opioid system plays a crucial role in stress-induced analgesia. Mu-opioid receptors (MORs), one of the major opioid receptors, are expressed widely in subpopulations of cells throughout the CNS. However, the potential roles of MORs expressed in glutamatergic (MOR_{Glut}) and γ-aminobutyric acidergic (MOR_{GABA}) neurons in stress-induced analgesia remain unclear. By examining tail-flick latencies to noxious radiant heat of male mice, here we investigated the contributions of MOR_{GABA} and MOR_{Glut} to behavioral analgesia and activities of neurons projecting from periaqueductal gray (PAG) to rostral ventromedial medulla (RVM) induced by a range of time courses of forced swim exposure. The moderate but not transitory or prolonged swim exposure induced a MOR-dependent analgesia, although all of these three stresses enhanced β-endorphin release. Selective deletion of MOR_{GABA} but not MOR_{Glut} clearly attenuated analgesia and blocked the enhancement of activities of PAG-RVM neurons induced by moderate swim exposure. Under transitory swim exposure, in contrast, selective deletion of MOR_{Glut} elicited an analgesia behavior via strengthening the activities of PAG-RVM neurons. These results indicate that MOR-dependent endogenous opioid signaling participates in nociceptive modulation in a wide range, not limited to moderate, of stress intensities. Endogenous activation of MOR_{GABA} exerts analgesia, whereas MOR_{Glut} produces antianalgesia. More importantly, with an increase of stress intensities, the efficiencies of MORs on nociception shifts from balance between MOR_{Glut} and MOR_{GABA} to biasing toward MOR_{GABA}-mediated processes. Our results point to the cellular dynamic characteristics of MORs expressed in excitatory and inhibitory neurons in pain modulation under various stress intensities.

Key words: forced swim stress; stress-induced analgesia; mu-opioid receptor; periaqueductal gray; β-endorphin

---

Significance Statement

Mu-opioid receptors (MORs) are one of the major opioid receptors playing a critical role in stress-induced analgesia and are widely expressed in different types of neurons, but their potential roles expressed in glutamatergic (MOR_{Glut}) and γ-aminobutyric acidergic (MOR_{GABA}) neurons are poorly understood. This work clarifies the divergent roles of MOR_{Glut} and MOR_{GABA} in analgesia under various swim stress intensities. We demonstrate that MOR_{GABA} neurons are essential for stress-induced analgesia, whereas MOR_{Glut} neurons elicit an anti-analgesic-like response. The contributions of MOR_{Glut} and MOR_{GABA} neurons to analgesia depends on stress intensity, their opposite effects neutralizing each other under transitory stress and then biasing them toward MOR_{GABA} under moderate stress. This report appraises different roles for the MORs in these neuronal populations in modulating opioid-dependent stress-induced analgesia.

Introduction

Stress-induced analgesia is an instinctive defensive reaction of mammals elicited by various acute stressful or negative stimuli, which can rapidly desensitize the pain response of the body and therefore dodge potential detriment in emergency circumstances like the fight-or-flight environment (Ferdousi and Finn, 2018). It is well demonstrated that stress-induced analgesia involves various neurotransmitters and neuropeptides, including opioids, cannabinoid, monoamine, GABA, and glutamate systems, leading to the activation of several intrinsic pain-suppressed mechanisms to produce analgesia. In particular, as critical pain regulators in CNS, endogenous opioid peptides (EOPs) energetically exert their antinociceptive effects by controlling the activation of the descending pain inhibitory pathway including the orbitofrontal cortex, the periaqueductal gray (PAG) of the midbrain, the rostral ventromedial medulla (RVM) of the brainstem, and the spinal cord dorsal horn in the processing of stress-induced analgesia (Gameiro et al., 2006; Butler and Finn, 2009).

Certain intensity of stress is required to induce opioid-dependent stress-induced analgesia. In general, moderate stress produces opioid analgesia and heavy stress produces nonopioid analgesia, whereas weak stress hardly produces any analgesic effect (Konecka et al., 1985; Miczek et al., 1985; Mogil et al., 1996). Several types of stressors in moderate intensity like restraint/immobilization, footshock or tailshock, forced swim, food and water deprivation, social isolation, and social conflict, that have been shown to trigger opioid-dependent stress-induced analgesia occur with naloxone (an opioid receptor antagonist) sensitivity (Konecka et al., 1985; Miczek et al., 1985; Menendez et al., 1993; Mogil et al., 1996; Larauche et al., 2012). Mu-opioid receptors (MORs), one of the four major opioid receptors encoded by *OPRM1* gene, play a critical role in opioid-dependent stress-induced analgesia (Fukunaga and Kishioka, 2000). Pharmacological and neurochemical studies have well demonstrated that either systemic or intracerebral and intrathecal administration of MORs blockage markedly reduced antinociception of rodents exposed in warm forced swim, intermittent footshock, and conditioned fear paradigms (Menendez et al., 1993; Mogil et al., 1996; Onodera et al., 2000; Wiedenmayer and Barr, 2000). Coincidentally, opioid-dependent stress-induced analgesia was significantly promoted by using selective MOR agonist systematically or intracerebrally (Calcagnetti et al., 1992; Vivian and Miczek, 1998). In addition, morphologic and biochemical studies have shown dense expressions of MORs in the core area of the descending pain inhibitory pathway (Stumm et al., 2004; Börner et al., 2007; Schnell and Wessendorf, 2008) and significant analgesic attenuation of opioid-dependent analgesia in MOR knockout mice (Rubinstein et al., 1996; LaBuda et al., 2000; Contet et al., 2006), providing further proof in demonstrating the vital roles of MORs on opioid-dependent stress-induced analgesia at a molecular level.

The expression of MOR-dependent stress-induced analgesia is closely associated with the elevated β-endorphin (β-EP) levels. β-EP, one of EOPs that has the highest binding affinity for MORs and is synthesized immediately in the early period of stress (Konecka et al., 1985; Tsigos and Chrousos, 2002; Smith and Vale, 2006; Bodnar, 2013; Pilozzi et al., 2020). The significant rise of β-EP concentrations in blood plasma and several pain-related brain areas like hypothalamus, pituitary gland, and PAG have been clearly observed in various stress paradigms including food and water deprivation and social conflict (Konecka et al., 1985; Külling et al., 1988). Mice with low β-EP sensitivity exhibit a decrease in pain threshold compared with normal β-EP sensitivity when exposed to swim stress (Lim and Funder, 1983). In addition, MOR-dependent stress-induced analgesia also can be weakened by exogenous administration of β-EP neutralizing antibody (Pilozzi et al., 2020). The contribution of β-EP in MOR-dependent stress-induced analgesia was further confirmed by using gene knockout technology, while forced swim stress-induced MOR-dependent analgesia was significantly abolished in β-EP-deleted mice (Parikh et al., 2011). However, it is worth noting that, under certain stress intensities, the enhanced β-EP was not accompanied by the expression of stress-induced analgesia (Konecka et al., 1985), and the mechanisms underlining the mismatch between β-EP concentration and analgesia remain unclear.

In the CNS, MORs are predominantly expressed in the axons, terminals, dendrites, and somata of GABAergic inhibitory interneurons spread over PAG and RVM. The activation of MORs is hypothesized to trigger the analgesic effects through suppression of inhibitory GABAergic inputs onto output neurons, which constitute the descending analgesic pathway, an indirect process of "GABA disinhibition" at the cellular level to activate the analgesic pathway (Drake and Milner, 2002; Lau and Vaughan, 2014). However, recent studies have also well clarified that in addition to GABAergic neurons, glutamatergic excitatory neurons also extensively expressed MORs throughout of the brain. Several pain-related areas, including prefrontal cortex, nucleus accumbens, thalamus, and PAG have considerable distribution of MORs in glutamatergic neurons (Schnell and Wessendorf, 2008; Zhang et al., 2020). This diversified distribution of MORs implies that the targets for β-EP to mediate MOR-dependent nociceptive modulation are not limited to GABAergic interneurons.

Copyright © 2022 Du et al.

Given the diversified distribution of MORs throughout pain-related pathways, here we supposed that MORs expressed in subpopulations of cells within the pain modulatory circuit fundamentally mediate opioid-dependent stress-induced analgesia through distinct cellular bases when undergoing different intensities of stress stimuli. To test this hypothesis, we developed two lines of MOR-knock-out mice that lacked MORs specifically in GABAergic inhibitory mice ($MOR_{GABA}^{-/-}$) and glutamatergic mice ($MOR_{Glut}^{-/-}$), respectively (Fan et al., 2019; Shi et al., 2020). By using selectively MOR deletion mice, combined with the pharmacological blockage method and fiber photometry recording, we exhibited a MOR-dependent stress-induced analgesia induced by different intensities of swim stress MOR_{GABA} and MOR_{Glut} deletion mice. Furthermore, the contributions of MOR_{GABA} and MOR_{Glut} on calcium activities of neurons projecting from PAG to RVM in stress-induced analgesia were further investigated.

Materials and Methods

Animals

All experiments with animals were performed in accordance with the Chinese Council on Animal Care and were approved by the Animal Care Committee of Shaanxi Normal University. One hundred and eight adult male C57BL/6J mice (from Model Animal Research Center, Nanjing University, Nanjing, People's Republic of China), 72 MOR mutant mice, and 48 littermate controls (Beijing Biocytogen) that were 10–12 weeks of age were used in this study. Seventy-two C57BL/6J mice were used for behavioral pharmacology, 24 were prepared for β-EP ELISA test, and others were administered a GCaMP adeno-associated virus (AAV) to serve as controls on fiber photometry recording. For MOR mutant mice, 24 were devoted to fiber photometry recording, others and 48 of their littermate controls were used for behavioral tests. Animal grouping in each part of the experiment was stated individually in the Results section. All animals were housed in groups of four in individually ventilated cages and maintained at $22 \pm 2°C$ and $55 \pm 5\%$ relative humidity under a normal 12 h light/dark cycle. Behavior experiments were conducted between 9:00 A.M. and 11:00 A.M. The animals were habituated for 5 d to acclimate to the environment and apparatus before behavioral experiments.

Mutant mouse lines were produced as below. Mice specifically lacking MORs in $MOR_{GABA}^{-/-}$ neurons or $MOR_{Glut}^{-/-}$ neurons were generated by crossing Oprm1 floxed mice to Gad2iCreERT2 mice or vGlut1iCreERT2 mice, respectively. The adult $Oprm1^{loxP/loxP}$:Gad2iCreERT2 or $Oprm1^{loxP/loxP}$:vGlut1iCreERT2 mice were treated with tamoxifen (2 mg/d, i.p.; Sigma-Aldrich) for 7 consecutive days to induce the deletion of MORs and were used for the experiments 2 weeks after the last injection. The littermates of Oprm1flox/flox:CreERT2$^{-/-}$ mice receiving similar tamoxifen treatment were taken as their control ($MOR_{GABA}^{+/+}$, $MOR_{Glut}^{+/+}$). To verify the deletion of MORs in the mutant mice, fluorescence in situ hybridization was used. The MOR_{GABA} deletions were verified in PAG (see Fig. 2A,B) and hippocampus (Shi et al., 2020). While PAG is lacking vGlut1-positive neurons (Soiza-Reilly and Commons, 2011), MOR_{Glut} deletions were verified in hippocampus (Shi et al., 2020) and anterior cingulate cortex (ACC), a major brain area sending vGlut1-positive projections to PAG (see Fig. 2C,D). The efficiency of the cell-type deletion of MORs was calculated (Fig. 2E,F).

Forced swim stress

Animals were placed individually in a cylindrical plastic container 30 cm in diameter and 45 cm in height. The level of the water ranged from 30 cm above the bottom of cylindrical plastic so as to avoid the escape of mice. The water temperature was maintained approximately $32 \pm 1°C$ in all experiments. The forced swim stress was induced by placing animals on the surface of the water for 1.5, 3, or 6 min. After stress, animals were carefully taken out from the plastic container and the surface moisture of skin was erased within 60 s to ensure that the skin condition was in accord with that of the prestress state.

Analgesia test

To examine the stress-induced analgesia, the tail-flick test was conducted before and immediately after swim exposure. Briefly, the animals were mildly restricted by a restrainer with their tail positioned in an apparatus (type YLS-12A, Shanghai Bio-will Co, Ltd.) for radiant heat stimulation on the surface of the tail. The tail-flick latency was defined as the time interval between the application of the radiant heat stimulation onto the tail and the abrupt removal of the tail from the nociceptive stimulus. The infrared wavelength of the radiant heat source was set at 805 nm, and the output power was set at 28 W, so that the baseline tail-flick latencies of the mice were controlled between 2 and 4 s. The cutoff time was set at 10 s to avoid tissue damage. For each animal, two sessions of tail-flick test, containing tail-flick latency before and after stress latency were conducted. Latency before stress was detected 120 min before swim stress, and latency after stress was tested immediately when the surface moisture of animal skin was dried after swim stress. Three measurements (with $\sim$60 s intervals) were taken from each session then averaged to determine tail-flick latency. Results were expressed as the percentage maximum possible effect (MPE), which was calculated as follows: MPE % = (poststress latency – prestress latency)/ (cutoff latency – prestress latency) $\times$ 100%.

Drugs

Saline (0.9%) and β-funaltrexamine [β-FNA (a MOR-specific antagonist); Sigma-Aldrich] were used to identify the influence of forced swim intensities on MOR-dependent forced swim stress-induced analgesia. Mice were treated with physiological saline or β-FNA dissolved in saline through subcutaneous injection with a dose of 40 mg/kg body weight 24 h before the stress and analgesia test. The volume of injection was set at 10 ml/kg.

Determination of serumal β-EP levels by ELISA

To detect the connection between swim stress intensities and β-EP levels, whole-blood samples were collected and

let it stand for ~20 h at 4°C, then the upper serum of blood was carefully sampled and stored in aliquot at −20°C before ELISA testing. At the time of detection, β-EP levels of serum were detected by using mouse β-EP ELISA Kit (lot JL10523-48T, J&L Biological).

AAV injection surgery

Animals were anesthetized with 4% isoflurane by immobilizing a chamber for small animals and then fixed with brain solid positioner with nonpuncturing ear bars. The 1% isoflurane was continuously delivered to nasopharynx of animals during surgery to maintain the anesthetic effect. Both eyes were smeared with eye ointment to avoid strong light stimulation and eye drying. After head hair was shaved and cranial dura mater was cut, retrograde transport GCaMP6f virus rAAV2/R-hsyn-GCaMP6f-WPRE-hGH-pA (300 nl/injection, 2.0×10^{12} copies/ml; BrainVTA) was injected into RVM of C57BL/6J, MOR$_{GABA}$$^{−/−}$, or MOR$_{Glut}$$^{−/−}$ mice by using a Hamilton microsyringe. To ensure the authenticity of GCaMP recording, rAAV2/R-hsyn-EYFP-WPRE-pA (300 nl/injection, 2.0×10^{12} copies/ml; BrainVTA) was also injected into C57BL/6J mice as a control. The injection site was used according to the mouse brain map: anteroposterior (AP), −5.80 mm; mediolateral (ML), 0 mm; dorsoventral (DV), −5.80 mm. After virus injection, the microsyringe was reserved in situ for 10 min, then the optical fiber ferrule was unilaterally inserted into PAG, according to the sites (AP, −4.80 mm; ML, 0.35 mm; DV, −2.80 mm) so that the calcium activities of neurons projecting from PAG to RVM could be monitored. Glass sonomer cement was finally smeared within the junction between the skull of animals and the optical fiber ferrule so as to strengthen the stability of the optical fiber ferrule. After surgery, all animals were housed at least 3 weeks before subsequent experiments.

Fiber photometry recording

To account for the calcium activities of neurons projecting from PAG to RVM, tail immersion of hot water was used as previously described (Moriya et al., 2020; Zhang et al., 2020). Animals were immobilized in the same restricted apparatus used for the tail-flick test with their tail exposed to receive the tail stimulation; and recording sessions of animals were also in sync with the tail-flick test, with basic calcium activities detected 120 min before stress, and poststress calcium activities recorded immediately when the surface moisture of animal skin was dried after swim stress. In the processing of fiber photometry recording, the root of the animal tail was immersed in 55°C hot water for 2 s to elicit calcium activities of projecting neurons, and 25°C water was set as its control. Each animal treated tail immersion three times with an interval of >60 s. In each stimulation, the "baseline windows" were defined as 5 s before each tail immersion, and the averaged fluorescence signal intensities within this time were denoted as F_0. The "event windows" were defined as 5 s after stimulus, and the averaged fluorescence signal intensities within this time were denoted as F_s. The environmental and systematic noises were recorded after disconnecting the tip of the fiber from an implanted

ceramic ferrule and blocking any optic input; these parts of averaged fluorescence signal intensities were denoted as F_n. The dynamics of the fluorescence signal intensities in stimuli were denoted as $\triangle F/F$ and calculated by computational formula: $\triangle F/F = F_s − F_0/F_0 − F_n$. The measuring result of each mice was the average of three times the calculated $\triangle F/F$. The sampling frequency was set at 50 Hz. Data were transferred and presented in MATLAB 2014.

Tissue preparation and fluorescence imaging

After recording, fluorescence imaging was used to detect the infection efficiency of AAV. Mice were deeply anesthetized with 25% urethane and transcardially perfused with normal saline and 4% dissolved in paraformaldehyde (PFA) and PBS successively. The brains were then taken out and postfixed in the same PFA PBS solution. Next, the brains were perfused with running water for at least 4 h and were soaked in a 30% sucrose PBS solution for 48 h at 4°C. Sections including PAG were finally sliced by using a cryostat (model CM 1950, Leica Biosystems) and imaged by fluorescence microscope (Zeiss USA).

Fluorescence *in situ* hybridization with RNAscope

The deletion of MORs in mutant mice was verified by fluorescence *in situ* hybridization assay (Fan et al., 2019; Shi et al., 2020). Briefly, mice were deeply anesthetized with isoflurane and killed by perfusion with 4°C saline (0.9%) within 5 min. The brains were quickly removed from the skulls and frozen on dry ice, and then embedded in OCT (catalog Tissue-Tek 4583, Sakura Finetek USA). Fresh frozen sections (16 μm) were made coronally with a freezing microtome (model CM1950, Leica Biosystems) and thaw mounted onto Superfrost Plus Microscope Slides (Thermo Fisher Scientific). The sections were fixed in 4% PFA for 60 min at 4°C before being dehydrated using graded ethanol (50%, 70%, and 100%) at room temperature for 5 min each and finally air dried. The sections were incubated with hydrogen dioxide for 10 min and subsequently pretreated with protease IV for 15 min. The probes for Oprm1 (16 synthetic oligonucleotides complementary to the nucleotide sequence 590–1458 of Oprm1), Gad2 (catalog #39371) and vglut1 (catalog #416631) were provided by Advanced Cell Diagnostics (ACD) and conjugated to Atto 594 and Atto 488, respectively. The procedure for *in situ* detection was performed using RNAscope Multiplex Fluorescent Reagent Kit version 2 (catalog #323100, ACD) according to the manufacturer instructions for fresh frozen tissue. After being heated with a HybEZTM oven (ACD) for 2 h, slides were mounted with the ProLong Gold Antifade Mountant (catalog #P10144, Thermo Fisher Scientific). Confocal images were captured with a fluorescence microscope (Zeiss), and cells with positive labeling were counted.

Statistical analysis

Data were presented as the mean ± SEM and were analyzed by using SPSS 22.0 software. Paired Student's *t* test, unpaired Student's *t* test, one-way ANOVA, and two-

way ANOVA were used, as stated individually in the Results section. The one-way ANOVAs were followed by a Dunnett's multiple-comparisons test. The two-way ANOVAs were followed by Sidak's multiple-comparisons test. The level of significance was set at $p < 0.05$ in all experiments.

Results

The involvement of β-EP and MORs in opioid-dependent stress-induced analgesia

Forced swim stress can steadily induce analgesic effects. Previous studies have shown that a 3 min swim exposure pattern in 32°C water causes opioid-dependent antinociception (Mogil et al., 1996), but the roles of MORs in this procedure are still unknown. To explore the contributions of MORs on forced swim stress-induced analgesia, β-FNA, a highly selective and irreversible MOR antagonist, was applied 24 h before the stress (Hayes et al., 1985; Banks, 2015). We examined the effect of transitory (1.5 min), moderate (3 min), and prolonged (6 min) forced swim stress on pain behaviors. Consistent with a previous study (Mogil et al., 1996), no analgesic effect was found in both saline-pretreated mice and β-FNA-pretreated mice after transitory swim exposure (drug treatment: $F_{(1,11)} = 0.7524$, $p = 0.4042$; stress: $F_{(1,11)} = 3.668$, $p = 0.0818$; interaction: $F_{(1,11)} = 0.7527$, $p = 0.4029$; two-way ANOVA; Fig. 1A); MPE percentage further revealed that β-FNA made little impact on pain behavior ($p = 0.6316$, unpaired Student's t test; Fig. 1A, right). However, saline-pretreated mice showed an obvious analgesia under moderate swim exposure, which could be dramatically attenuated by β-FNA pretreatment shown in both tail-flick latencies (drug treatment: $F_{(1,11)} = 8.396$, $p = 0.0145$; stress: $F_{(1,11)} = 95.08$, $p = 0.0000$; interaction: $F_{(1,11)} = 13.82$, $p = 0.0034$; two-way ANOVA; Fig. 2B) and MPE percentage ($p = 0.0004$, unpaired Student's t test; Fig. 1B, right). In addition, a significant analgesic effect was shown in both saline-pretreated mice under prolonged swim exposure (drug treatment: $F_{(1,11)} = 0.04057$, $p = 0.8440$; stress: $F_{(1,11)} = 55.39$, $p = 0.0000$; interaction: $F_{(1,11)} = 0.0084$, $p = 0.9204$; two-way ANOVA; Fig. 1C), and MPE percentage showed insignificance between two groups ($p = 0.8922$, unpaired Student's t test; Fig. 1C, right). These results indicate a secondary analgesic role of MORs in prolonged swim stress.

To test whether MORs are endogenously activated by EOPs after stress, the levels of β-EP, an EOP with high binding affinity for MORs in forced swim stress (Parikh et al., 2011), was tested by ELISA. Surprisingly, remarkable differences of serum β-EP levels were exhibited among distinct stress intensities ($F_{(3,20)} = 4.982$, $p = 0.0096$, one-way ANOVA; Fig. 1D), and significant increases were found in all of the forced swim exposures compared with control mice ($p = 0.0429$ for transitory swim; $p = 0.0094$ for moderate swim; $p = 0.0090$ for prolonged swim), though there was no analgesic effect following transitory swim exposure (Fig. 1A). Therefore, our results indicate that all transitory, moderate, and prolonged swim exposures can activate the endogenous opioid system, but only moderate swim exposure induces the expression of MOR-dependent analgesic behavior.

The contributions of MORs expressed in glutamatergic and GABAergic neurons to stress-induced analgesia

The MORs are expressed not only in inhibitory neurons but also excitatory neurons, and both of them are involved in pain modulation. To address the distinct effects of MORs in glutamatergic (MOR_{Glut}) and GABAergic (MOR_{GABA}) neurons on analgesia under transitory or moderate swim exposure, two mice lines specifically lacking, respectively, MOR_{GABA} ($MOR_{GABA}^{-/-}$) and MOR_{Glut} ($MOR_{Glut}^{-/-}$) were used. The deletion of MORs in the mutant mice was verified by using RNAscope (Fig. 2). No significant difference in the basal tail-flick latency was detected between mice with MOR deletions and their wild-type littermates, respectively ($p > 0.05$, unpaired Student's t tests). However, a diverse modulation of MORs on the analgesic effect related to stress intensities were found in those mouse lines.

After transitory swim exposure, both $MOR_{GABA}^{-/-}$ mice and their littermates still exhibited nondetectable change of the tail-flick latencies (genotype: $F_{(1,11)} = 0.0705$, $p = 0.7955$; stress: $F_{(1,11)} = 2.959$, $p = 0.1134$; interaction: $F_{(1,11)} = 0.2043$, $p = 0.6601$; two-way ANOVA; Fig. 3A, left) and MPE percentage ($p = 0.7433$, unpaired Student's t test; Fig. 3A, right). However, the tail-flick latencies of $MOR_{Glut}^{-/-}$ mice were significantly increased after stress, whereas no significant changes were seen in their wild-type littermates (genotype: $F_{(1,11)} = 4.874$, $p = 0.0494$; stress: $F_{(1,11)} = 20.61$, $p = 0.0008$; interaction: $F_{(1,11)} = 9.890$, $p = 0.0093$; two-way ANOVA; Fig. 3B, left). Meanwhile, the MPE percentage of these two groups displayed a significant difference ($p = 0.0059$, unpaired Student's t test; Fig. 3B, right), implying the involvement of MOR_{Glut} on pain mediation under transitory swim exposure.

Under moderate swim exposure, although the tail-flick latencies of both $MOR_{GABA}^{-/-}$ mice and their littermates showed significant increase after stress, the increased magnitude of latency from $MOR_{GABA}^{-/-}$ mice was much inhibited, compared with their littermates (genotype: $F_{(1,11)} = 4.118$, $p = 0.0673$; stress: $F_{(1,11)} = 59.37$, $p = 0.0000$; interaction: $F_{(1,11)} = 20.76$, $p = 0.0008$; two-way ANOVA; Fig. 3C, left). The MPE percentage also exhibited a significant difference between groups ($p = 0.0023$, unpaired Student's t test; Fig. 3C, right), although the tail-flick latencies of both genotype mice were significantly increased. In contrast, the tail-flick latencies of both $MOR_{Glut}^{-/-}$ mice and their littermates showed almost the same degree of increase after stress (genotype: $F_{(1,11)} = 3.005$, $p = 0.1109$; stress: $F_{(1,11)} = 51.37$, $p = 0.0000$; interaction: $F_{(1,11)} = 0.0578$, $p = 0.8144$; two-way ANOVA; Fig. 3D, left), and the MPE percentage also exhibited insignificant differences between the groups ($p = 0.6357$, unpaired Student's t test; Fig. 3D, right). These results indicate a predominant contribution of MOR_{GABA} to analgesia under moderate swim exposure, though their additional analgesic components involved in this stress-induced analgesia paradigm could not be excluded.
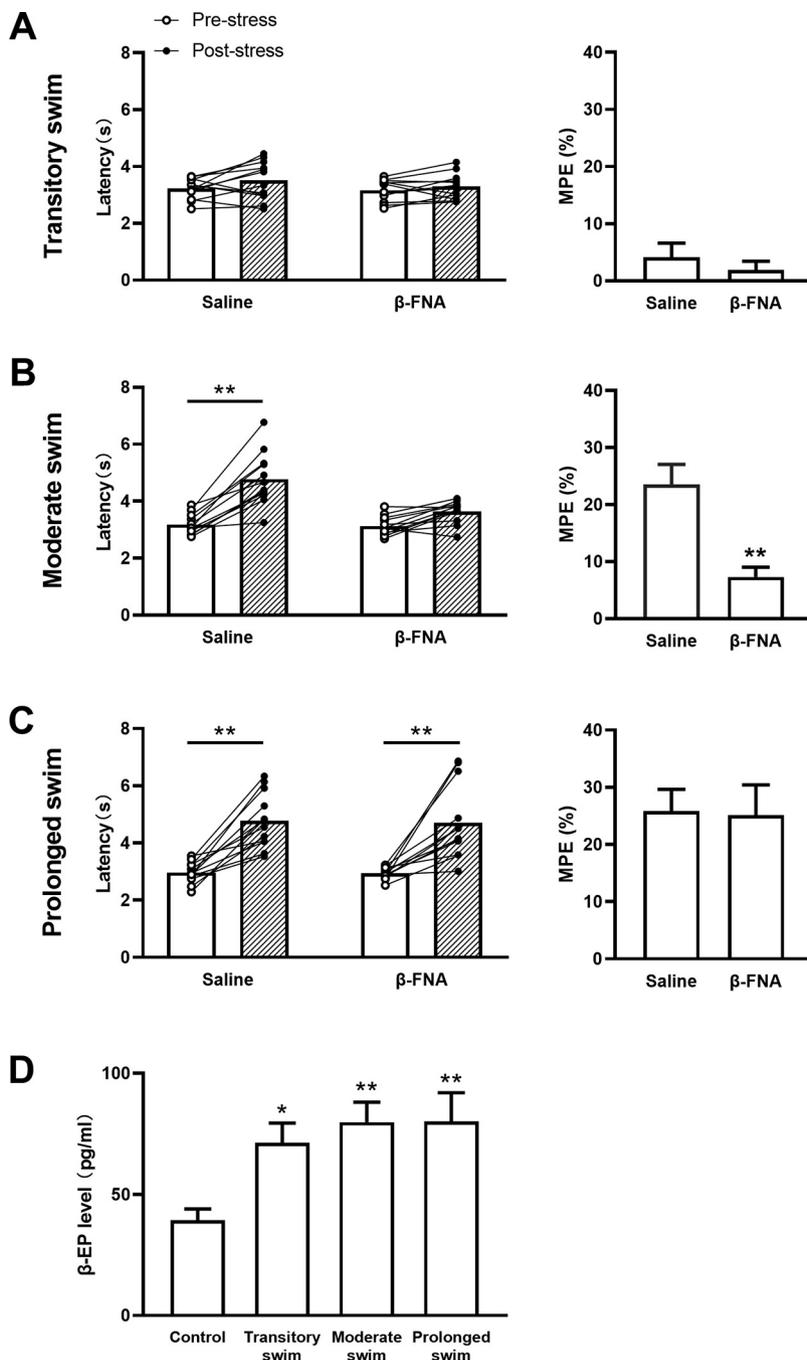
Figure 1. The involvement of β-EP and MORs on opioid-dependent stress-induced analgesia. **A–C**, Left, Tail-flick latency under transitory swim (**A**), moderate swim (**B**), or prolonged swim (**C**) exposure in mice pretreated with saline or β-FNA; $n = 12$ for each group, **$p < 0.01$. Right, Equated MPE percentage from left groups, with data shown as the mean ± SEM. **$p < 0.01$ versus saline. **D**, β-EP levels in serum analysis using ELISA. $n = 6$ for each group, data are shown as mean ± SEM. *$p < 0.05$; **$p < 0.01$ versus control.

Thus, our results reveal an opposite modulation of the MOR_{Glut} and MOR_{GABA} on stress-induced analgesia. The activation of MOR_{GABA} produces analgesia, whereas MOR_{Glut} elicits anti-analgesic-like effects. Furthermore, the functional balance between MOR_{Glut} and MOR_{GABA} on pain modulation could be broken depending on stress intensity.

Activation of PAG–RVM-projecting neurons responding to thermal noxious stimulus

In the descending pain inhibitory pathway, the activation of neurons projecting from PAG to RVM play a crucial role for stress-induced analgesia. To investigate the impacts of swim exposure on the activities of PAG–RVM-projecting neurons, *in vivo* calcium signals
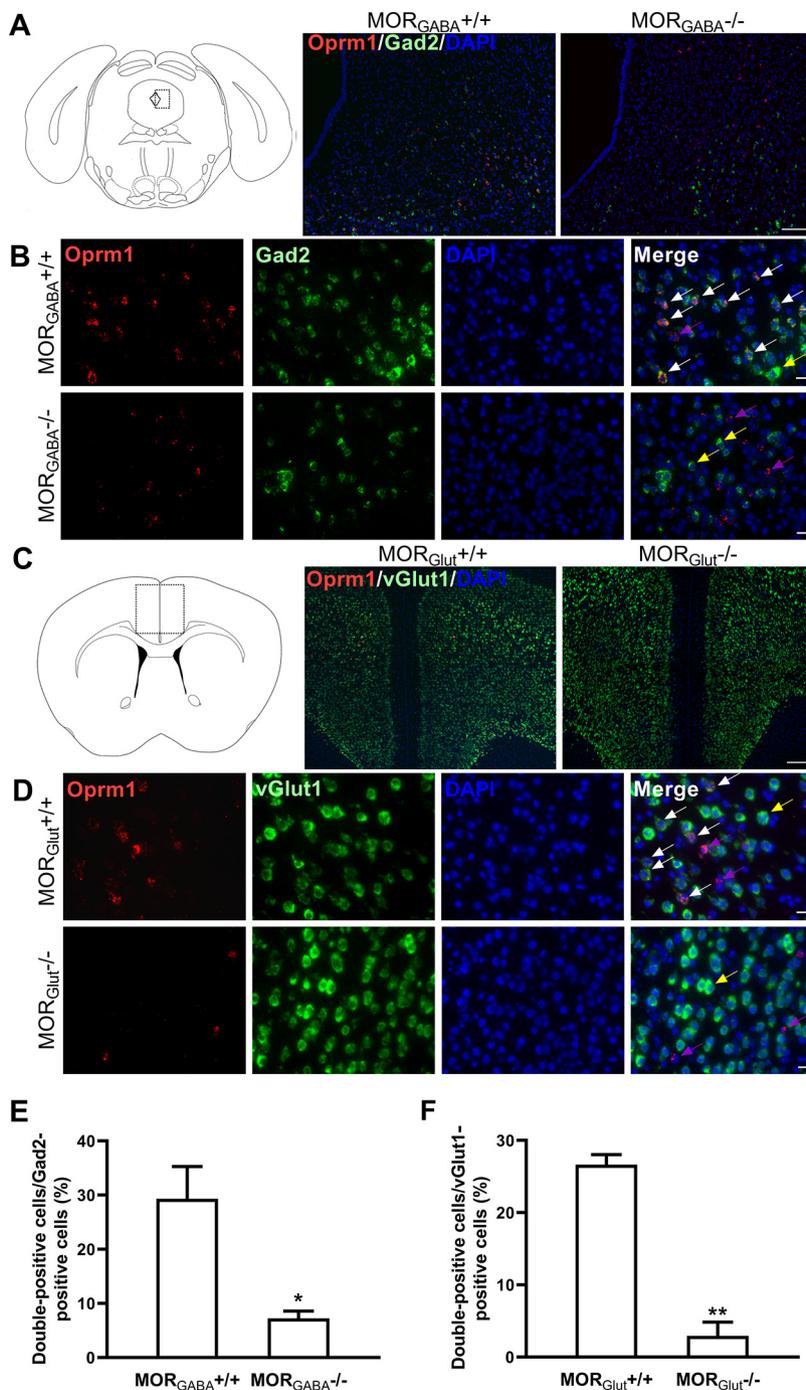
Figure 2. Generation of conditional knock-out mice specifically lacking MORs on glutamatergic and GABAergic neurons. *A*, Schematic of *in situ* hybridization for *Oprm1* mRNA and *GAD2* mRNA in the PAG areas in $\text{MOR}_{\text{GABA}}^{+/+}$ and $\text{MOR}_{\text{GABA}}^{-/-}$ mice. The nucleus is stained in blue (DAPI), *GAD2* mRNA is stained in green, and *Oprm1* mRNA is stained in red. Scale bar, 100 μm. *B*, Higher-magnification images of the fields in the PAG areas in $\text{MOR}_{\text{GABA}}^{+/+}$ and $\text{MOR}_{\text{GABA}}^{-/-}$ mice. The white arrowhead indicates a double-labeled cell with *Oprm1* mRNA and *GAD2* mRNA; the purple arrowheads represent *Oprm1* mRNA localization in *GAD2*-negative cells; and the yellow arrowheads represent *GAD2*-positive cells without *Oprm1* mRNA. Scale bar, 20 μm. *C*, Schematic of *in situ* hybridization for *Oprm1* mRNA and *vGlut1* mRNA in the ACC areas in $\text{MOR}_{\text{Glut}}^{+/+}$ and $\text{MOR}_{\text{Glut}}^{-/-}$ mice. The nucleus is stained in blue (DAPI), *vGlut1* mRNA is stained in green, and *Oprm1* mRNA is stained in red. Scale bar, 200 μm. *D*, Higher-magnification images of the fields in the ACC areas in $\text{MOR}_{\text{Glut}}^{+/+}$ and $\text{MOR}_{\text{Glut}}^{-/-}$ mice. The white arrowhead indicates a double-labeled cell with *Oprm1* mRNA and *vGlut1* mRNA; the purple arrowheads represent *Oprm1* mRNA localization in *vGlut1*-negative cells; and the yellow arrowheads represent *vGlut1*-positive cells without *Oprm1* mRNA. Scale bar, 20 μm. *E*, Quantitative analysis of the percentage of double-positive neurons (*Oprm1* and *GAD2*) against the *GAD2*-positive neurons. *$p < 0.05$ versus $\text{MOR}_{\text{GABA}}^{+/+}$, unpaired *t* test ($n = 3$ in each group). *F*, Quantitative analysis of the percentage of double-positive neurons (*Oprm1* and *vGlut1*) against the *vGlut1*-positive neurons. **$p < 0.01$ versus $\text{MOR}_{\text{Glut}}^{+/+}$, unpaired *t* test ($n = 3$ in each group).
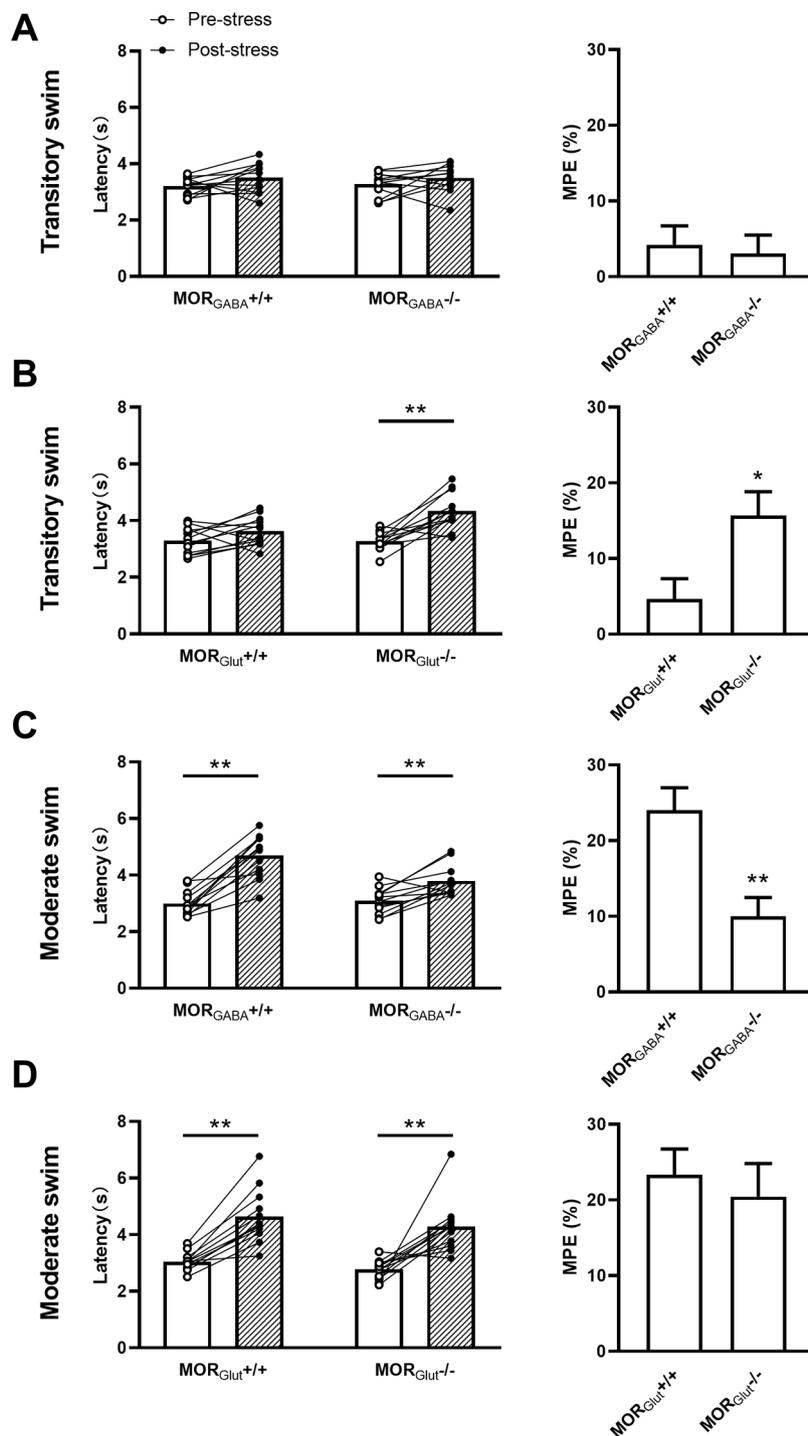
Figure 3. *A–D*, The contributions of MORs expressed in glutamatergic (*B*, *D*) and GABAergic (*A*, *C*) neurons to stress-induced analgesia under transitory (*A*, *B*) or moderate (*C*, *D*) swim exposure. Left, Tail-flick latency. Right, Equated MPE percentage; $n = 12$ for each group; data are shown as the mean ± SEM. **$p < 0.01$.

of those cells were tested by injecting the retrograde transport GCaMP6f virus or virus enhanced yellow fluorescent protein (EYFP; as control) into RVM, which axoplasmic transported from axons in RVM to somata in PAG (Fig. 4A). The availability of GCaMP6f expressions in RVM and PAG were confirmed by histologic method (Fig. 4A).

Previous studies have well demonstrated that the pain modulatory projections have the ability to respond to and tackle nociceptive information (Samineni et al., 2019; Huang et al., 2020; Moriya et al., 2020; Zhang et al., 2020). To verify that the nociceptive information has the ability to activate PAG–RVM-projecting neurons, their responses to thermal noxious stimulus (55°C water) or
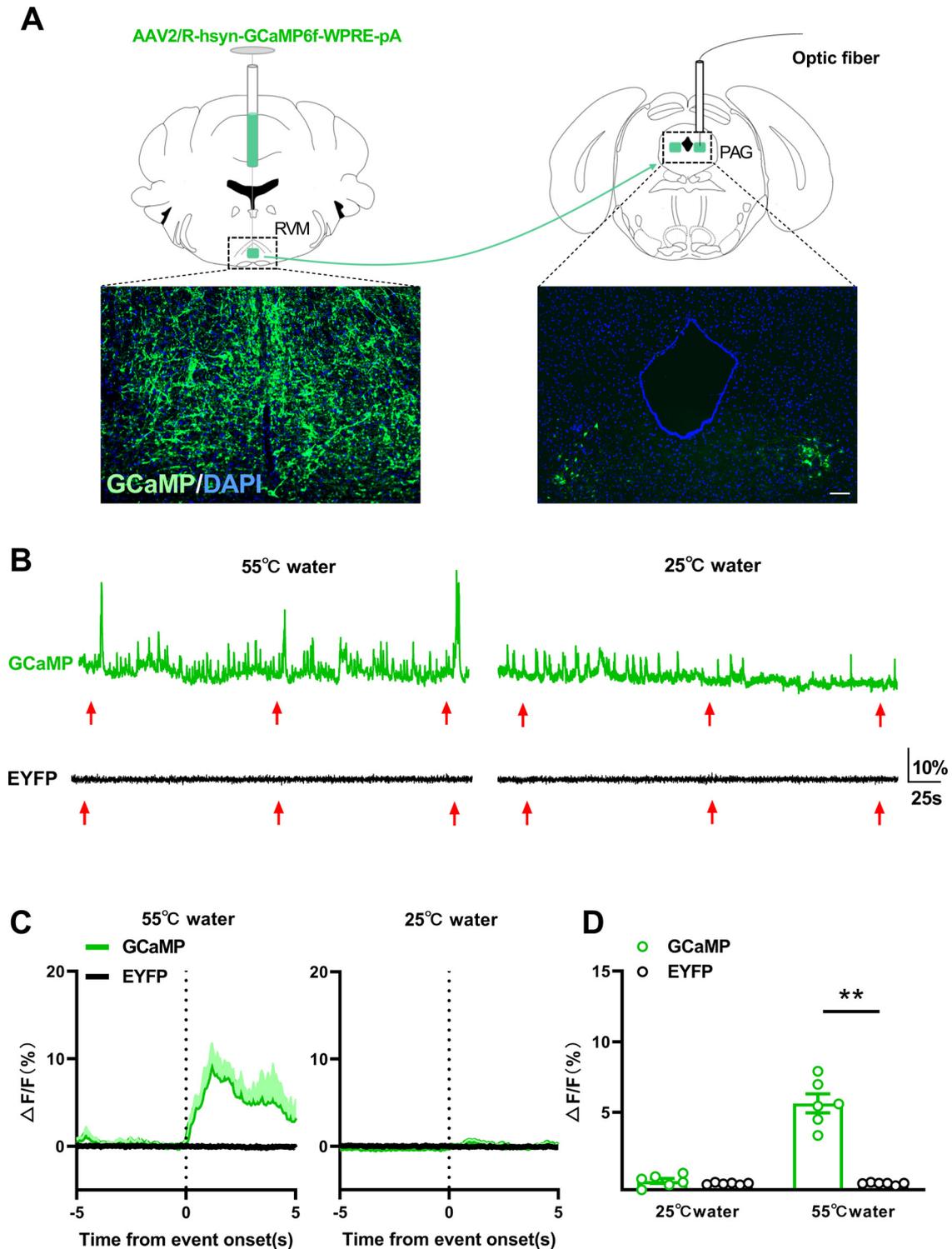
Figure 4. The responses of PAG-RVM neurons to thermal stimulus. **A**, Schematic representation of the virus injection sites and optic fiber insertion sites, and corresponding schematic of GCaMP expression on RVM and PAG. Scale bar, 100 μm. **B**, Typically representative photometry traces from GCaMP (top) or EYFP (bottom) mouse relative to the onset in response to 55°C (left) and 25°C (right) water tail immersion. Each red arrow represents an event (tail immersion stimulus). **C**, Time course of the averaged fluorescence signal change in response to tail immersion. Light-colored shadow indicates the SEM; $n = 6$ for each group. **D**, Comparison of the averaged fluorescence signal change between EYFP and GCaMP groups during the onset period (0–5 s) for each stimulation. **$p < 0.01$.

thermal innocuous stimulus (25°C water) were monitored by recording the fluorescence intensities.

On the background of spontaneous fluorescence signals, which indicated that there are tonic activities of PAG–RVM neurons under the basal condition, mice treated with GCaMP virus exhibited a large magnitude of fluorescence signals in response to thermal noxious stimulus but not to thermal innocuous stimulus (Fig. 4B, C). No fluorescence responses to either of the two stimuli were observed in EYFP mice, indicating that these detectable fluorescence signals during thermal noxious stimulation are not because of movement artifact (Fig. 4B,C). The analysis (two-way ANOVA; Fig. 4D) of averaged fluorescence responses during event windows (0–5 s after thermal stimulus) in each session revealed a significant difference of virus ($F_{(1,5)} = 93.63$, $p = 0.0002$) and stimulus ($F_{(1,5)} = 115.5$, $p = 0.0001$), and a significant interaction between virus and stimulus ($F_{(1,5)} = 70.68$, $p = 0.0004$). Subsequent Sidak's multiple-comparisons test revealed that there was a significant difference of fluorescence intensities between thermal noxious and innocuous stimuli in GCaMP mice ($p = 0.0004$), and a significant difference between GCaMP and EYFP mice under 55°C water stimulus ($p = 0.0003$), indicating that PAG-RVM neurons are specifically involved in the handling of thermal noxious information.

The effects of MOR$_{Glut}$ and MOR$_{GABA}$ on activities of PAG–RVM-projecting neurons under different stress intensities

Next, we investigated the influence of stress on activities of PAG-RVM neurons responding to thermal stimulus. Consistent with behavioral results, after transitory swim exposure, fluorescence intensities of PAG–RVM-projecting neurons responding to thermal noxious stimulus in wild-type mice were almost unaltered, compared with that of prestress (Fig. 5A). In contrast, MOR$_{Glut}$$^{-/-}$ mice exhibited an obvious enhancement of fluorescence intensities after stress (Fig. 5C), and, surprisingly, fluorescence intensities of MOR$_{GABA}$$^{-/-}$ mice were decreased in poststress (Fig. 5B) without change of behavioral performance (Fig. 3A). The further analysis of averaged fluorescence intensities during event windows revealed an insignificant difference between prestress and poststress in wild-type mice ($p = 0.7404$, paired Student's t test; Fig. 5D), and a significant decrease in MOR$_{GABA}$$^{-/-}$ mice ($p = 0.0112$, paired Student's t test; Fig. 5E), but a significant increase in MOR$_{Glut}$$^{-/-}$ mice ($p = 0.0379$, paired Student's t test; Fig. 5F), respectively. These results suggest that MORs expressed in both GABAergic neurons and glutamatergic neurons are indeed involved in pain modulation under transitory swim exposure, and exhibit opposite effects on activities of PAG-RVM neurons in the descending pain inhibitory pathway.

On the other hand, after moderate swim exposure, the response of PAG-RVM neurons to thermal stimulus from both wild-type and MOR$_{Glut}$$^{-/-}$ mice increased remarkably (Fig. 6A,C). However, this increased response was lacking in MOR$_{GABA}$$^{-/-}$ mice (Fig. 6B). The analysis of averaged fluorescence intensities during event windows

revealed that there were significant increases in fluorescence signal in both wild-type mice ($p = 0.0079$, paired Student's t test; Fig. 6D) and MOR$_{Glut}$$^{-/-}$ mice ($p = 0.0138$, paired Student's t tests; Fig. 6F), but not in MOR$_{GABA}$$^{-/-}$ mice ($p = 0.9799$, paired Student's t test; Fig. 6E) after stress. These results imply that, under moderate swim exposure, the enhanced activities of PAG-RVM neurons from wild-type mice can mainly be attributed to the activation of MOR$_{GABA}$, which covers the opposite effects of MOR$_{Glut}$ to inhibit activities of PAG-RVM neurons.

Discussion

Here, we illuminated the opposite contributions of MOR$_{Glut}$ and MOR$_{GABA}$ on analgesia induced by various intensities of forced swim stress. The activation of MOR$_{GABA}$ produces analgesia, whereas MOR$_{Glut}$ tends to elicit anti-analgesic-like effects. Furthermore, the effects of these two MORs in distinct subpopulations of neurons on pain modulation showed a dynamic character in responding to stress intensity: with progressive enhancement of stress intensity, the efficiencies of MORs on nociception shifts from balance between MOR$_{Glut}$ and MOR$_{GABA}$ to biasing toward MOR$_{GABA}$-mediated disinhibition, and finally to loss of efficacy.

Stress-induced analgesia is a pain-inhibitory reaction usually occurs during or following exposure to sudden environmental change in nature. Although the numbers of neurotransmitter and neuromedin are involved in this physiological process, the opioid-dependent mechanism is still considered as a critical constituent part of stress-induced analgesia (Konecka et al., 1985; Miczek et al., 1985; Menendez et al., 1993; Mogil et al., 1996; Larauche et al., 2012). Our present study used 32°C forced swim paradigm, a classic stress procedure to induce analgesia, in a range of time courses to investigate the contributions of MORs to stress-induced analgesia. After transitory swim exposure, a significant increase of β-EP levels (Fig. 1D) was detected without accompanying behavioral analgesia (Fig. 1A). Surprisingly, MOR$_{Glut}$$^{-/-}$ mice exhibited an obvious stress-induced analgesia, together with an enhancement of activities of PAG-RVM neurons responding to noxious stimulus. Thus, both MOR$_{Glut}$ and MOR$_{GABA}$ were endogenously activated by weak stress stimulus but played counteractive effects on analgesic modulation: activation of MOR$_{GABA}$ tended to induce analgesia, whereas that of MOR$_{Glut}$ was inclined to exert a anti-analgesic-like effect, and these two opposite effects on PAG-RVM neurons neutralized each other and no analgesic behaviors was observed (Fig. 7).

In contrast, a steadily stress-induced analgesia depending mainly on MORs was observed after moderate swim exposure, as supported by the evidence of further elevated β-EP (Fig. 1D) and the effect of MOR antagonist β-FNA (Fig. 1B). This MOR-dependent analgesia mainly relies on endogenous activation of MOR$_{GABA}$ because selective deletion of MOR$_{GABA}$ inhibited stress-induced analgesia in the same direction as did β-FNA administration. On the contrary, selective deletion of MOR$_{Glut}$ did not affect stress-induced analgesia, indirectly showing an overwhelming electivity of MOR$_{GABA}$
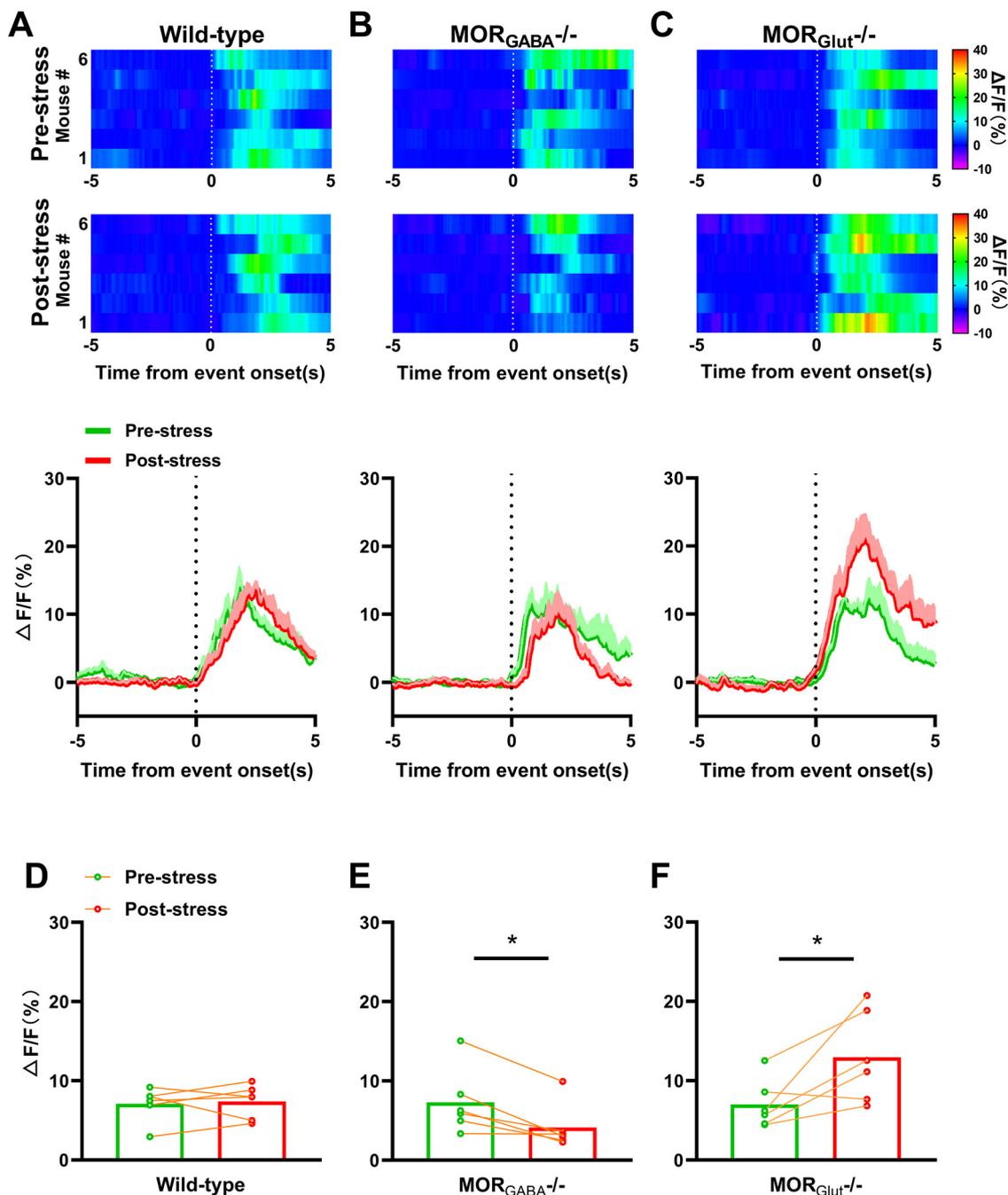
Figure 5. Changes in fluorescence intensities of PAG-RVM neurons induced by thermal stimulus under transitory swim exposure. *A–C*, Top, Heat map of averaged fluorescence dynamics of GCaMP relative to the onset prestress and poststress in response to 55°C water tail immersion on wild-type, $MOR_{GABA}^{-/-}$, or $MOR_{Glut}^{-/-}$ mice; $n = 6$ for each group. Bottom, Time course of the averaged fluorescence intensities prestress and poststress on wild-type, $MOR_{GABA}^{-/-}$, or $MOR_{Glut}^{-/-}$ groups. *D–F*, Comparison of the averaged fluorescence intensities between prestress and poststress during the onset period (0–5 s) for each stimulation on wild-type, $MOR_{GABA}^{-/-}$, and $MOR_{Glut}^{-/-}$ mice. *$p < 0.05$.

on stress-induced analgesia in this condition. With the functional enhancement of endogenous opioids in parallel with the increase in stress intensity, the effects of MOR_{GABA} hold a dominant position, even covering the influence of MOR_{Glut}, on pain modulation. Thus, a prominently analgesic effect mainly elicited by MOR_{GABA} was highlighted in the behavioral test, and an enhancement

of PAG-RVM neuron activation was observed. Therefore, our present study showed a shift of MOR effects from balance between excitatory glutamatergic neurons and inhibitory GABAergic neurons to biasing toward inhibitory GABAergic neurons, in accordance with stress intensity (Fig. 7). While prolonging the swim time, MORs no longer mediated stress-induced analgesia, suggesting that
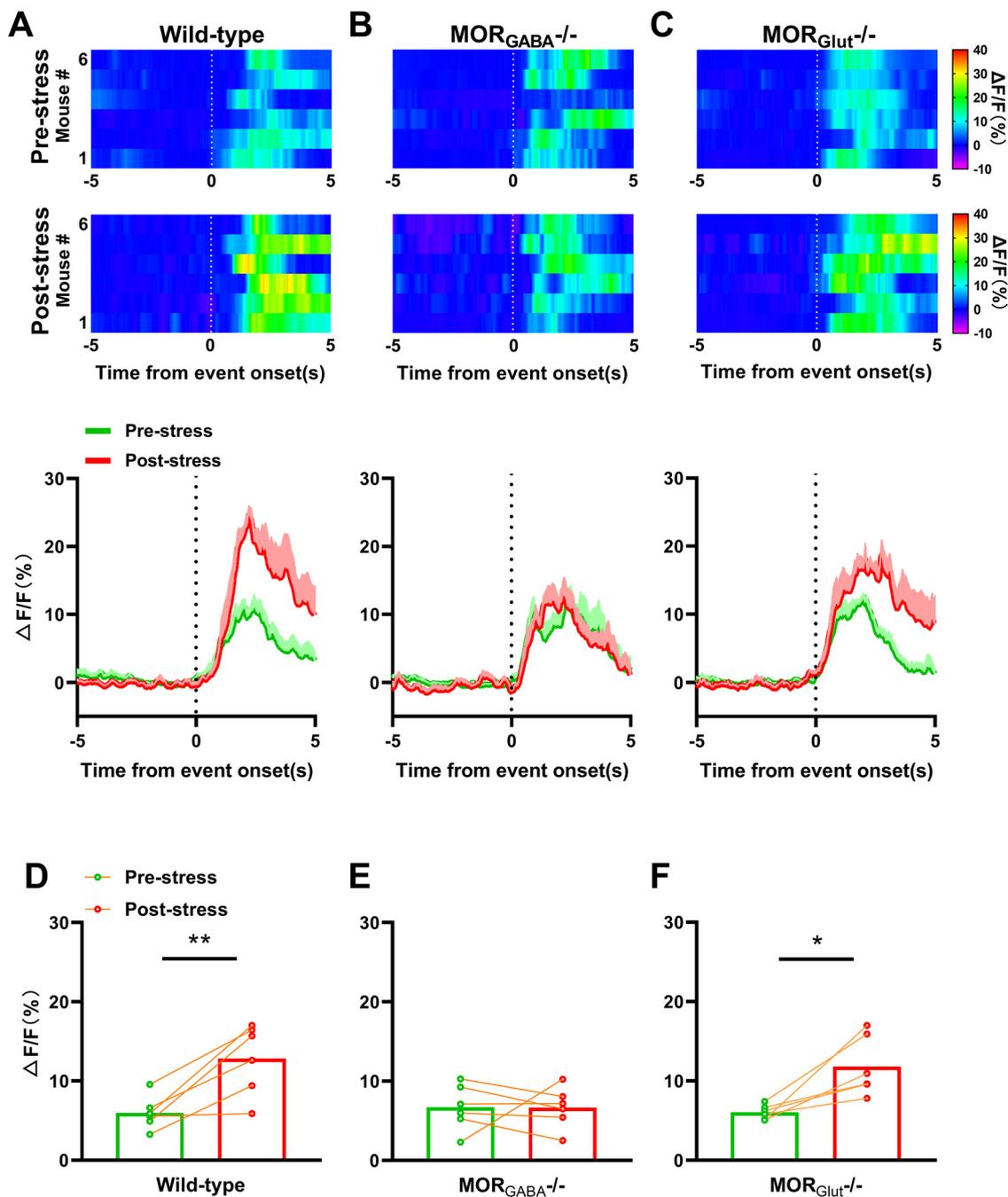
Figure 6. Changes in the fluorescence intensities of PAG-RVM neurons induced by thermal stimulus under moderate swim exposure. **A–C**, Top, Heat map of averaged fluorescence dynamics of GCaMP relative to the onset prestress and poststress in response to 55°C water tail immersion on wild-type, $MOR_{GABA}{}^{-/-}$, or $MOR_{Glut}{}^{-/-}$ mice; $n = 6$ for each group. Bottom, Time course of the averaged fluorescence intensities prestress and poststress on wild-type, $MOR_{GABA}{}^{-/-}$, or $MOR_{Glut}{}^{-/-}$ groups. **D–F**, Comparison of the averaged fluorescence intensities between prestress and poststress during the onset period (0–5 s) for each stimulation on wild-type, $MOR_{GABA}{}^{-/-}$, and $MOR_{Glut}{}^{-/-}$ mice. *$p < 0.05$, **$p < 0.01$.

the endogenous opioid system lost the initiative of analgesia under heavy stress.

β-EP is involved in stress responses and is closely related to stress-induced analgesia. It is clear that the hypothalamic–pituitary–adrenal (HPA) axis is the first activated neural circuit in response to stress events, and β-EP secretion is fully mediated by activation of the HPA axis. The

transcriptional and translational levels of β-EP are significantly increased when the release of corticotropin-releasing hormone induced by activation of the HPA axis (Tsigos and Chrousos, 2002). In addition, β-endorphinergic neurons in the CNS are extensively projected into a pain-mediated area including hippocampus, pituitarium, and brainstem, and the delivered β-EP is highly degradation
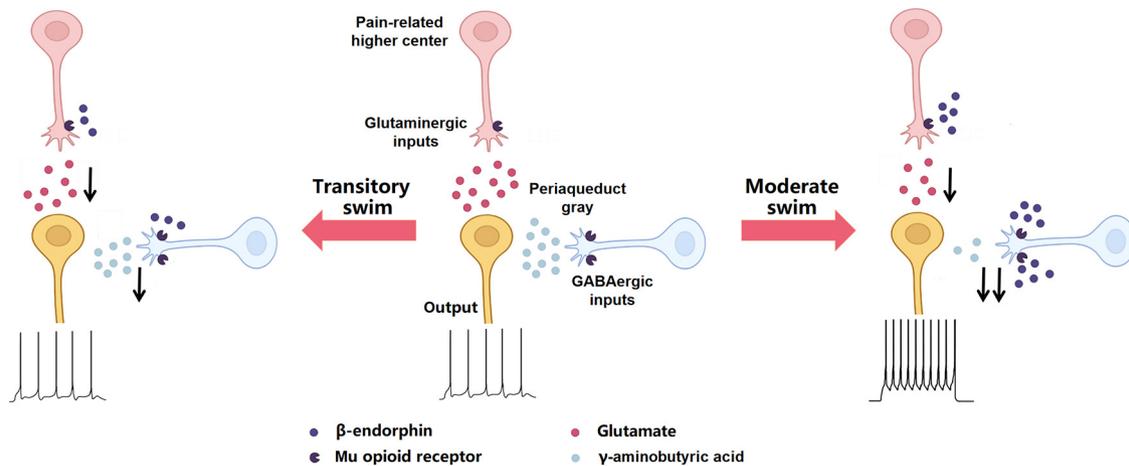
Figure 7. Schematic illustration showing the proposed mechanism of the contributions of MOR$_{GABA}$ and MOR$_{Glut}$ to analgesia induced by different intensities of stress. Under transitory swim stress, the activation of MOR$_{Glut}$ and MOR$_{GABA}$ by the released β-endorphin equally inhibits glutamatergic and GABAergic inputs on PAG-RVM neurons, respectively. These opposite effects on PAG-RVM neurons should neutralize each other and keeps the activity of PAG-projecting neurons almost unchanged. In contrast, under moderate swim stress, MOR$_{GABA}$ are further activated by the more elevated β-endorphin to cause imbalance of excitatory–inhibitory synaptic inputs on PAG neurons, and therefore leads to disinhibition of PAG-RVM neurons and induces analgesia.

resistant in the brain (Smyth, 2016). Therefore, β-EP can be immediately secreted and distributed throughout the brain and blood vessels at the early stages of stress events and exerts its biological function over a considerable period. However, the present study showed a conflicting result that a significant increase of β-EP levels in plasma did not follow with expected analgesia under transitory swim exposure (Fig. 1*A*,*D*). In fact, the mismatch between the expression of opioid-dependent analgesia and enhancement levels of β-EP occurs frequently in several stress paradigms (Scallet, 1982; Izquierdo et al., 1984; Konecka et al., 1985; Külling et al., 1988). Just 24 h of food deprivation could significantly promote concentrations of β-EP twice the basal level in mice blood plasma, whereas significant analgesia needs food deprivation for 48 h without a further change in β-EP concentration (Konecka et al., 1985). In addition, MOR-dependent analgesia induced by social conflict needs aggressive confrontation between two populations of mice, but mere exposure of a test mouse to a nonaggressive opponent also provokes the changing of β-EP levels in pain-related brain areas (Külling et al., 1988). A similar phenomenon can be found in aversive sound and conditioned fear stress. The analgesia exhibited is hysteresis by the time β-EP levels have already elevated (Scallet, 1982; Izquierdo et al., 1984). Our results provide a potential explanation from another perspective for the mismatch between analgesia and β-EP: the neutralizing effects of MOR$_{Glut}$ and MOR$_{GABA}$, although further investigations are required for the distinct mechanisms.

The various expressions of MORs in glutamatergic and GABAergic neurons have clearly been identified recently, and both of them are oppositely involved in pain modulation with distinct mechanisms (Zhang et al., 2020). It was suggested that the exogenous opioid-induced analgesia is mediated by MOR$_{Glut}$, whereas the endogenous opioid-induced analgesia is mediated by MOR$_{GABA}$ (Zhang et al., 2020). Our present study genetically manipulated

MORs expressed in glutamatergic or GABAergic neurons and found that, although transitory swim exposure failed to trigger remarkable analgesia in wild-type and MOR$_{GABA}$$^{-/-}$ mice, MOR$_{Glut}$$^{-/-}$ mice exhibited significant analgesic effect after stress stimulus. Previous studies about pain modulation of glutamatergic neuron MORs have mainly concentrated on exogenous opioid drug-induced pain modulatory effects (Kemp et al., 1996; Wang et al., 2018; Zhang et al., 2020). Based on the morphologic evidence that *vGlut2*-positive rather than *vGlut1*-positive neurons are densely distributed on brainstem and spinal cord (Soiza-Reilly and Commons, 2011), it has been verified that MORs expressed in *vGlut2*-positive neurons strongly inhibit pain signal transduction at the spinal level, but barely have effects on endogenous opioid-induced analgesia (Zhang et al., 2020). However, MORs are also extensively expressed in *vGlut1*-positive neurons at pain-related higher centers like primary and secondary somatosensory cortex, ACC, and hippocampus (Shi et al., 2020; Zhang et al., 2020), and they project to downstream pain-related areas of brainstem like PAG (Basbaum and Fields, 1984). Our present study indicated that MORs in *vGlut1*-positive neurons are also involved in endogenous opioid-induced pain modulation and, other than exogenous opioid-dependent analgesic effects at spinal level, they exhibit a novel anti-analgesic-like effects under the transitory forced swim paradigm. These results suggest a cell subtype specificity of glutamatergic neuron MORs on pain modulation.

By contrast, moderate forced swim paradigm-induced analgesia was significantly decreased in MOR$_{GABA}$$^{-/-}$ mice but was impervious in MOR$_{Glut}$$^{-/-}$ mice, indicating that the main mediation of analgesia is accomplished by GABAergic neuron MORs under this condition. This is consistent with the GABA disinhibition hypothesis of stress-induced analgesia (Yeung et al., 1977; Behbehani

and Fields, 1979; Basbaum and Fields, 1984). Activation of MORs expressed on GABAergic neurons are suggested to attenuate their inhibition of the descending pain inhibitory pathway in brainstem or excitatory neurons projecting to the descending pain inhibitory pathway at prefrontal cortex and hippocampus, so that analgesia was induced (Lau and Vaughan, 2014).

In the CNS, modulation of stress-induced analgesia is mainly accomplished by the activation of the descending pain inhibitory pathway (Bourne et al., 2014; Kwon et al., 2014; Huang et al., 2019; Holgersen et al., 2021). The descending pain inhibitory pathway consists of PAG, RVM, and spinal dorsal horn. Activation of this circuit abolishes nociceptive transmission from dorsal horn of the spinal cord to supraspinal pain-related brain areas, resulting in inhibition of nociceptive signaling and antinociceptive effects (Bourne et al., 2014; Kwon et al., 2014; Ferdousi and Finn, 2018; Huang et al., 2019). As the origin of the descending pain pathway, neurons projecting from PAG to RVM play a vital role in the collection of nociceptive information from forebrain and the mediation of endogenous analgesia (Heinricher, 2016; Chen and Heinricher, 2019). MORs are generally located at the axons, terminals, dendrites, and somata of neurons (Drake and Milner, 2002) to depress the firing rate and neurotransmitter release of neurons by a G-protein-mediated inhibition process (Drake and Milner, 2002). Thus, endogenous activation of MOR_{Glut} inhibits the pain-related excitatory inputs to the descending pain pathway, whereas the activation of MOR_{GABA} disinhibits this circuit. Based on the extensive distributions of both GABAergic and glutamatergic neuron MORs on the descending pain pathway and pain-related higher brain areas projecting to this circuit, respectively, we evaluated the changes of PAG-RVM neuron activities by detecting calcium signals under transitory or moderate swim exposure to further investigate cell type-based differential MORs-mediated stress-induced analgesia. The enhancement of calcium activities on nociceptive neurons under thermal or mechanical noxious stimulus has been reported in several studies (Samineni et al., 2019; Huang et al., 2020; Moriya et al., 2020; Zhang et al., 2020), and efficient involvement of these projection neurons in the mediation of thermal noxious stimulus was verified in the present study.

Under transitory swim exposure, the calcium activities of PAG-RVM neurons poststress were unchanged in wild-type mice, but were significantly increased in $MOR_{Glut}^{-/-}$ mice and obviously decreased in $MOR_{GABA}^{-/-}$ mice (Fig. 5), suggesting that both MOR_{Glut} and MOR_{GABA} are involved in transitory swim exposure stress and exhibit an oppositely mediated effect in the descending pain inhibitory pathway. The activation of MORs expressed in GABAergic neurons elicits "disinhibition" of PAG-RVM neurons to induce analgesia, as it is uncovered by MOR_{Glut} deletion (Fig. 6C,F). In contrast, the activation of MORs expressed in glutamatergic neurons inhibits PAG-RVM neurons to cause antianalgesia, as it is uncovered by MOR_{GABA} deletion (Fig. 6B,E). Taking one with another, the opposite effects of MORs on the

activities of PAG-RVM neurons through these two cell-type neurons might be neutralized (Fig. 7), so we did not detect a significant change of both tail-flick test and calcium activities in wild-type mice. This might be one reason to explain the inconsistency between elevated β-EP levels and missed analgesia in the behavioral test.

By contrast, under moderate swim exposure, the activities of PAG-RVM neurons in both wild-type and $MOR_{Glut}^{-/-}$ mice exhibited significant enhancements, whereas those in $MOR_{GABA}^{-/-}$ mice showed a lack of this enhancement, revealing a prominent effect of MOR_{GABA}-mediated GABA disinhibition in the descending analgesic pathway on forced swim stress-induced analgesia (Lau and Vaughan, 2014). Under this stress condition, the inhibitory effect of MOR_{Glut} on PAG-RVM neurons was remarkably overwhelmed by the disinhibitory effect of MOR_{GABA}; therefore, the descending pain inhibitory pathway was activated, and behavioral analgesia was detected (Fig. 7). Although electrophysiological evidence is still lacking to support that GABA disinhibition mechanism in acute stress is the major source of MOR-dependent analgesia, our results provide a new perspective to investigate the role of GABAergic neuron MORs on pain modulation pathways at cellular levels. However, the distinct mechanisms underlying the shifted weight of MOR_{Glut} and MOR_{GABA} efficiencies on the descending pain inhibitory pathway in response to different stress intensities remain speculative. It seems that the amount of β-EP related to stress intensity and the asymmetric distribution of MORs on glutamatergic and GABAergic neurons in the descending inhibitory pathway might serve as a key parameters to modulate the descending inhibitory pathway.

Strangely, transitory swim exposure did not induce obvious analgesia in $MOR_{GABA}^{-/-}$ mice, but calcium activities of PAG-RVM neurons was significantly weakened. This inconsistency between behavioral performance and the activities of PAG-RVM neurons might be attributed to the character of the descending pain inhibitory pathway, because it is a pain information modulatory circuit rather than a pain information transmittal circuit (Bourne et al., 2014; Kwon et al., 2014; Huang et al., 2019). Previous pharmacological research has already clarified that lidocaine, a sodium-channel blocker untouched by MORs, attenuated the chronic allodynia of mice through local administration into PAG and RVM, whereas they have no effect on tail-flick latency in healthy mice with the same treatment (Pertovaara et al., 1996). So, inhibition of the descending pain inhibitory pathway will not produce a direct hyperalgesic effect.

Overall, our present study highlighted the roles of MORs expressed in different populations of cells on MOR-dependent analgesia underwent various intensities of stress. However, the distinct mechanisms underlying the shifts of MOR_{Glut} and MOR_{GABA} efficiencies responding to stress intensity remain to be further explored. In addition, given that acute stress induces sex differences of analgesia in both laboratory animals and humans (Mogil, 2012), our present study of males should not

generalize to females. It is worth investigating whether the sex-specific modulation of MORs in pain processing is involved in the present study.

References

Banks WA (2015) Peptides and the blood-brain barrier. Peptides 72:16–19.

Basbaum AI, Fields HL (1984) Endogenous pain control systems: brainstem spinal pathways and endorphin circuitry. Annu Rev Neurosci 7:309–338.

Behbehani MM, Fields HL (1979) Evidence that an excitatory connection between the periaqueductal gray and nucleus raphe magnus mediates stimulation produced analgesia. Brain Res 170:85–93.

Bodnar RJ (2013) Endogenous opiates and behavior: 2012. Peptides 50:55–95.

Börner C, Stumm R, Höllt V, Kraus J (2007) Comparative analysis of mu-opioid receptor expression in immune and neuronal cells. J Neuroimmunol 188:56–63.

Bourne S, Machado AG, Nagel SJ (2014) Basic anatomy and physiology of pain pathways. Neurosurg Clin N Am 25:629–638.

Butler RK, Finn DP (2009) Stress-induced analgesia. Prog Neurobiol 88:184–202.

Calcagnetti DJ, Stafinsky JL, Crisp T (1992) A single restraint stress exposure potentiates analgesia induced by intrathecally administered DAGO. Brain Res 592:305–309.

Chen Q, Heinricher MM (2019) Descending control mechanisms and chronic pain. Curr Rheumatol Rep 21:13.

Contet C, Gavériaux-Ruff C, Matifas A, Caradec C, Champy MF, Kieffer BL (2006) Dissociation of analgesic and hormonal responses to forced swim stress using opioid receptor knockout mice. Neuropsychopharmacology 31:1733–1744.

Drake CT, Milner TA (2002) Mu opioid receptors are in discrete hippocampal interneuron subpopulations. Hippocampus 12:119–136.

Fan KM, Qiu LJ, Ma N, Du YN, Qian ZQ, Wei CL, Han J, Ren W, Shi MM, Liu ZQ (2019) Acute stress facilitates LTD induction at glutamatergic synapses in the hippocampal CA1 region by activating μ-opioid receptors on GABAergic neurons. Front Neurosci 13:71.

Ferdousi M, Finn DP (2018) Stress-induced modulation of pain: role of the endogenous opioid system. Prog Brain Res 239:121–177.

Fukunaga Y, Kishioka S (2000) Enkephalinergic neurons in the periaqueductal gray and morphine withdrawal. Jpn J Pharmacol 82:175–180.

Gameiro GH, Gameiro PH, da Silva Andrade A, Pereira LF, Arthuri MT, Marcondes FK, Veiga MC (2006) Nociception- and anxiety-like behavior in rats submitted to different periods of restraint stress. Physiol Behav 87:643–649.

Hayes AG, Skingle M, Tyers MB (1985) Effect of beta-funaltrexamine on opioid side-effects produced by morphine and U-50, 488H. J Pharm Pharmacol 37:841–843.

Heinricher MM (2016) Pain modulation and the transition from acute to chronic pain. Adv Exp Med Biol 904:105–115.

Holgersen EM, Gandhi S, Zhou Y, Kim J, Vaz B, Bogojeski J, Bugno M, Shalev Z, Cheung-Ong K, Gonçalves J, O'Hara M, Kron K, Verby M, Sun M, Kakaradov B, Delong A, Merico D, Deshwar AG (2021) Transcriptome-wide off-target effects of steric-blocking oligonucleotides. Nucleic Acid Ther 31:392–403.

Huang J, Gadotti VM, Chen L, Souza IA, Huang S, Wang D, Ramakrishnan C, Deisseroth K, Zhang Z, Zamponi GW (2019) A neuronal circuit for activating descending modulation of neuropathic pain. Nat Neurosci 22:1659–1668.

Huang S, Zhang Z, Gambeta E, Xu SC, Thomas C, Godfrey N, Chen L, M'Dahoma S, Borgland SL, Zamponi GW (2020) Dopamine inputs from the ventral tegmental area into the medial prefrontal cortex modulate neuropathic pain-associated behaviors in mice. Cell Rep 31:107812.

Izquierdo I, Souza DO, Dias RD, Perry ML, Carrasco MA, Volkmer N, Netto CA (1984) Effect of various behavioral training and testing procedures on brain β-endorphin-like immunoreactivity and the possible role of β-endorphin in behavioral regulation. Psychoneuroendocrinology 9:381–389.

Kemp T, Spike RC, Watt C, Todd AJ (1996) The μ-opioid receptor (MOR1) is mainly restricted to neurons that do not contain GABA or glycine in the superficial dorsal horn of the rat spinal cord. Neuroscience 75:1231–1238.

Konecka AM, Sroczynska I, Przewlocki R (1985) The effect of food and water deprivation on post-stress analgesia in mice and levels of beta-endorphin and dynorphin in blood plasma and hypothalamus. Arch Int Physiol Biochim 93:279–284.

Külling P, Frischknecht HR, Pasi A, Waser PG, Siegfried B (1988) Social conflict-induced changes in nociception and β-endorphin-like immunoreactivity in pituitary and discrete brain areas of C57BL/6 and DBA/2 mice. Brain Res 450:237–246.

Kwon M, Altin M, Duenas H, Alev L (2014) The role of descending inhibitory pathways on chronic pain modulation and clinical implications. Pain Pract 14:656–667.

LaBuda CJ, Sora I, Uhl GR, Fuchs PN (2000) Stress-induced analgesia in μ-opioid receptor knockout mice reveals normal function of the δ-opioid receptor system. Brain Res 869:1–5.

Larauche M, Mulak A, Kim YS, Labus J, Million M, Taché Y (2012) Visceral analgesia induced by acute and repeated water avoidance stress in rats: sex difference in opioid involvement. Neurogastroenterol Motil 24:1031–e547.

Lau BK, Vaughan CW (2014) Descending modulation of pain: the GABA disinhibition hypothesis of analgesia. Curr Opin Neurobiol 29:159–164.

Lim AT, Funder JW (1983) Stress-induced changes in plasma, pituitary and hypothalamic immunoreactive beta-endorphin: effects of diurnal variation, adrenalectomy, corticosteroids, and opiate agonists and antagonists. Neuroendocrinology 36:225–234.

Menendez L, Andres-Trelles F, Hidalgo A, Baamonde A (1993) Opioid footshock-induced analgesia in mice acutely falls by stress prolongation. Physiol Behav 53:1115–1119.

Miczek KA, Thompson ML, Shuster L (1985) Naloxone injections into the periaqueductal grey area and arcuate nucleus block analgesia in defeated mice. Psychopharmacology (Berl) 87:39–42.

Mogil JS (2012) Sex differences in pain and pain inhibition: multiple explanations of a controversial phenomenon. Nat Rev Neurosci 13:859–866.

Mogil JS, Sternberg WF, Balian H, Liebeskind JC, Sadowski B (1996) Opioid and nonopioid swim stress-induced analgesia: a parametric analysis in mice. Physiol Behav 59:123–132.

Moriya S, Yamashita A, Masukawa D, Kambe Y, Sakaguchi J, Setoyama H, Yamanaka A, Kuwaki T (2020) Involvement of supralemniscal nucleus (B9) 5-HT neuronal system in nociceptive processing: a fiber photometry study. Mol Brain 13:14.

Onodera K, Sakurada S, Furuta S, Yonezawa A, Arai K, Hayashi T, Katsuyama S, Sato T, Miyazaki S, Kisara K (2000) Differential involvement of opioid receptors in stress-induced antinociception caused by repeated exposure to forced walking stress in mice. Pharmacology 61:96–100.

Parikh D, Hamid A, Friedman TC, Nguyen K, Tseng A, Marquez P, Lutfy K (2011) Stress-induced analgesia and endogenous opioid peptides: the importance of stress duration. Eur J Pharmacol 650:563–567.

Pertovaara A, Wei H, Hämäläinen MM (1996) Lidocaine in the rostroventromedial medulla and the periaqueductal gray attenuates allodynia in neuropathic rats. Neurosci Lett 218:127–130.

Pilozzi A, Carro C, Huang X (2020) Roles of β-endorphin in stress, behavior, neuroinflammation, and brain energy metabolism. Int J Mol Sci 22:338.

Rubinstein M, Mogil JS, Jpnón M, Chan EC, Allen RG, Low MJ (1996) Absence of opioid stress-induced analgesia in mice lacking beta-endorphin by site-directed mutagenesis. Proc Natl Acad Sci U|S|A 93:3995–4000.

Samineni VK, Grajales-Reyes JG, Sundaram SS, Yoo JJ, Gereau RW (2019) Cell type-specific modulation of sensory and affective components of itch in the periaqueductal gray. Nat Commun 10:4356.

Scallet AC (1982) Effects of conditioned fear and environmental novelty on plasma β-endorphin in the rat. Peptides 3:203–206.

Schnell SA, Wessendorf MW (2008) Coexpression of the mu-opioid receptor splice variant MOR1C and the vesicular glutamate transporter 2 (VGLUT2) in rat central nervous system. J Comp Neurol 508:542–564.

Shi MM, Fan KM, Qiao YN, Xu JH, Qiu LJ, Li X, Liu Y, Qian ZQ, Wei CL, Han J, Fan J, Tian YF, Ren W, Liu ZQ (2020) Hippocampal μ-opioid receptors on GABAergic neurons mediate stress-induced impairment of memory retrieval. Mol Psychiatry 25:977–992.

Smith SM, Vale WW (2006) The role of the hypothalamic-pituitary-adrenal axis in neuroendocrine responses to stress. Dialogues Clin Neurosci 8:383–395.

Smyth DG (2016) 60 YEARS OF POMC: lipotropin and beta-endorphin: a perspective. J Mol Endocrinol 56:T13–T25.

Soiza-Reilly M, Commons KG (2011) Glutamatergic drive of the dorsal raphe nucleus. J Chem Neuroanat 41:247–255.

Stumm RK, Zhou C, Schulz S, Höllt V (2004) Neuronal types expressing mu- and delta-opioid receptor mRNA in the rat hippocampal formation. J Comp Neurol 469:107–118.

Tsigos C, Chrousos GP (2002) Hypothalamic–pituitary–adrenal axis, neuroendocrine factors and stress. J Psychosom Res 53:865–871.

Vivian JA, Miczek KA (1998) Effects of mu and delta opioid agonists and antagonists on affective vocal and reflexive pain responses during social stress in rats. Psychopharmacology (Berl) 139:364–375.

Wang D, Tawfik VL, Corder G, Low SA, François A, Basbaum AI, Scherrer G (2018) Functional divergence of delta and mu opioid receptor organization in CNS pain circuits. Neuron 98:90–108.e5.

Wiedenmayer CP, Barr GA (2000) Mu opioid receptors in the ventrolateral periaqueductal gray mediate stress-induced analgesia but not immobility in rat pups. Behav Neurosci 114:125–136.

Yeung JC, Yaksh TL, Rudy TA (1977) Concurrent mapping of brain sites for sensitivity to the direct application of morphine and focal electrical stimulation in the production of antinociception in the rat. Pain 4:23–40.

Zhang XY, Dou YN, Yuan L, Li Q, Zhu YJ, Wang M, Sun YG (2020) Different neuronal populations mediate inflammatory pain analgesia by exogenous and endogenous opioids. Elife 9:e55289.